


Spring 2015

# Structural elucidation of AggR-activated regulator, aar, in enteroaggregative Escherichia coli

Andrew Heindel  
*James Madison University*

Follow this and additional works at: <https://commons.lib.jmu.edu/honors201019>

 Part of the [Biochemistry Commons](#), and the [Structural Biology Commons](#)

---

## Recommended Citation

Heindel, Andrew, "Structural elucidation of AggR-activated regulator, aar, in enteroaggregative Escherichia coli" (2015). *Senior Honors Projects, 2010-current*. 54.  
<https://commons.lib.jmu.edu/honors201019/54>

This Thesis is brought to you for free and open access by the Honors College at JMU Scholarly Commons. It has been accepted for inclusion in Senior Honors Projects, 2010-current by an authorized administrator of JMU Scholarly Commons. For more information, please contact [dc\\_admin@jmu.edu](mailto:dc_admin@jmu.edu).

Structural Elucidation of AggR-activated Regulator, Aar, in Enteroaggregative *Escherichia coli*

---

An Honors Program Project Presented to  
the Faculty of the Undergraduate  
College of Science and Mathematics  
James Madison University

---

by Andrew Joseph Heindel

May 2015

---

Accepted by the faculty of the Department of Biology, James Madison University, in partial fulfillment of the requirements for the Honors Program.

FACULTY COMMITTEE:

HONORS PROGRAM APPROVAL:

---

Project Advisor: Nathan T. Wright, Ph.D  
Assistant Professor, Chemistry and Biochemistry

---

Philip Frana, Ph.D.,  
Interim Director, Honors Program

---

Reader: Christopher E. Berdsen, Ph.D  
Assistant Professor, Chemistry and Biochemistry

---

Reader: Gina MacDonald, Ph.D  
Professor, Chemistry and Biochemistry

---

PUBLIC PRESENTATION

This work is accepted for presentation, in part or in full, at Chemistry Spring Symposium on March 26, 2015.

## Table of Contents

Table of Contents	2
List of Figures	3
Acknowledgements	4
Abstract	5
Introduction	6
Materials and Methods	11
Results	14
Discussion	19
References	21
Supplemental Methods	23
Supplemental Results	23

## List of Figures

Prevalence of Diarrheagenic <i>E. coli</i>	7
Phylogenic Analysis of Aar	9
SDS-PAGE of Ubiquitin-Aar	14
Representative CD Spectra	15
Ubiquitin-Aar CD Spectra	15
HPLC/MS	17
Fractional Separation and SDS-PAGE	18

## **Acknowledgements**

I would like to thank Dr. Nathan Wright for his guidance and assistance. I would also like to thank Dr. Christopher Berndsen, Dr. Oleksandr Kokhan and Dr. Gina MacDonald for assistance with laboratory equipment. Funding for this project was provided by 4VA.

## Abstract

Travelers' Diarrhea is the number one cause of childhood death in the world. Enteroaggregative Escherichia coli (EAEC) is one of the main causes of this disease. EAEC adhere to the surface of the intestine and stack in a brick-like pattern. Via an unstudied quorum-sensing mechanism, these bacteria express a variety of virulence factors that lead to diarrhea. The long-term goal of this research is to elucidate the mechanism by which EAEC changes from benign to virulent. A previously-unstudied open-reading frame in EAEC, AggR activated repressor (Aar), has recently been hypothesized to act as one of the major transcription factors influencing virulence. Here, we describe two viable methods for purification and a method for cleavage. Circular dichroism (CD) data suggests a partially  $\alpha$ -helical structure. Further tests, including multi-dimensional NMR and X-ray crystallography, are currently being conducted to determine the tertiary structure of the protein.

## Introduction

Diarrhea is a condition that produces three or more loose or liquid stools in a 24 hour period. Although diarrhea affects adults and children, the severity of the disease in children is far greater. According to the World Health Organization (WHO), diarrhea is the leading causes of mortality and morbidity in the world, killing roughly 760,000 children per year under the age of five (World Health Organization, 2014). Most children experience diarrhea due to pathogenic bacterial species like *Escherichia coli* (*E. coli*).

Diarrhea can be induced by bacterial infections. According to the Centers for Disease control, six different pathogenic strains of *E. coli* exist, Shiga toxin-producing (STEC), Enterotoxigenic (ETEC), Enteropathogenic (EPEC), Enteroinvasive (EIEC), Diffusely adherent (DAEC) and Enteroaggregative (EAEC) (Centers for Disease Control [CDC], 2014). All pathotypes utilize adhesion proteins to line the mucosal walls of the intestines (Kaper, Nataro, & Harry, 2004). EIEC utilizes mechanical mechanisms to induce symptoms (Van Den Beld & Reubsaet, 2012). STEC, ETEC, EPEC, DIEC and EAEC contain additional genes that produce enterotoxins, increasing Cl<sup>-</sup> permeability (Stark & Duncan, 1972). This results in Ca<sup>2+</sup> and H<sub>2</sub>O leakage into the lumen (Stark & Duncan, 1972). Although these five pathotypes have similar severities, the prevalence of EAEC is far greater than that of STEC, ETEC, EPEC and DIEC in children.

The prevalence of EAEC in young populations is highlighted by a study conducted in Mongolia between 2001 and 2002. Sarantuya *et al.* collected 238 *E. coli* isolates from children, aged zero to 16, with sporadic diarrhea (> three watery stools a day) and 278 *E. coli* isolates from apparently healthy children (Sarantuya *et al.*, 2004). The results of cultured stool samples indicated four different pathotypes of diarrheagenic *E. coli*: ETEC, EPEC, EIEC and EAEC.

However, the incidence of EAEC (15.1%) was far higher than the incidence of any other pathotype (0 to 6%) in the entire cohort (Sarantuya *et al.*, 2004). More importantly, the group examined the incidence of EAEC between the diarrheal population and the control population. The percentage of EAEC was greater in the diarrheal group (36%) than the control group (16%)( $p < 0.0006$ ) (Table 1), suggesting that EAEC can be a pathogenic species of bacteria (Sarantuya *et al.*, 2004). Sarantuya *et al.* also collected data about AggR, a virulence factor commonly found in the genome of pathogenic EAEC. As indicated in Table 1, AggR is more common in the diarrheal group (19%) than in the non-diarrheal group (4%) ( $p < 0.0004$ ) (Sarantuya *et al.*, 2004). These data suggest that AggR likely contributes to pathogenicity of EAEC (Sarantuya *et al.*, 2004).

**Table 1.** Prevalence of diarrheagenic *E. coli* categories of among *E. coli* strains examined in Mongolian cohort (Sarantuya *et al.*, 2004).

DEC category <sup>a</sup>	No. of strains (%)		P value <sup>b</sup>	O serotypes <sup>c</sup> (no. of strains)
	Diarrheal (n = 238)	Control (n = 278)		
EPEC (total)	9 (3.8)	0 (0)	0.0009	
Typical	5 (2.1)	0 (0)	0.02	O55 (1), O111 (3), NT (1)
Atypical	4 (1.6)	0 (0)	0.04	O6 (1), O111 (1), NT (2)
ETEC (total)	14 (6.0)	3 (1.1)	0.002	
LT only	5 (2.1)	1 (0.3)	NS	O143 (1), O159 (1), NT (4)
ST only	8 (3.3)	1 (0.3)	0.013	O6 (1), O78 (1), NT (7)
LT and ST	1 (0.4)	1 (0.3)	NS	O55 (1), NT (1)
EIEC	8 (3.3)	0 (0)	0.002	O28 (1), O112 (1), O115 (1), O158 (1), NT (4)
EHEC	0 (0)	1 (0.3)	NS	NT (1)
EAEC (total)	36 (15.1)	16 (5.7)	0.0006	
AggR positive	19 (8.0)	4 (1.4)	0.0004	O15 (2), O126 (2), O148 (1), NT (18)
AggR negative	17 (7.1)	12 (4.3)	NS	NT (29)
Total	67 (28.1)	20 (7.2)	<0.0001	

<sup>a</sup> LT, heat-labile toxin; ST, heat-stable toxin.

<sup>b</sup> NS, not significant.

<sup>c</sup> NT, nontypeable.

Several studies have highlighted a strong relationship between the presence of AggR and diarrheal disease (Boisen *et al.*, 2014; Sarantuya *et al.*, 2004). This relationship has led to multiple AggR characterization studies. Unpublished data by Nataro *et al.* suggested that there was a positive correlation between AggR and aggregative adherence fimbria (AAF/I). The relationship was probed to determine if AggR controlled AAF/I expression. AggR-knockout and



wildtype cells were subjected to immunogold electron microscopy (Nataro, Yikang, Yingkang, & Walker, 1994). AggR-knockouts lacked observable fimbria in the images, while the wildtype cell contained visible fimbria (Nataro et al., 1994). Additional studies confirmed that AggR controls transcription of AAF/I (Nataro et al., 1994). Protein homology studies also suggest that AggR is a member of the AraC/XylS family of transcriptional regulators, alluding to its transcriptional control potential (Nataro et al., 1994). Regulon characterization also determined at least 44 other genes under AggR transcriptional control (Morin, Santiago, Ernst, Guillot, & Nataro, 2013). Sixteen of these genes are part of the Aai T6SS system, responsible for protein transport across membranes (Morin et al., 2013). Five genes are part of the dispersin secretion system, responsible for a surface coat that acts to disperse bacteria, and four genes are part of the AAF/II fimbrial biogenesis system, responsible for fimbria production (Morin et al., 2013). In a separate study, Morin *et al.* concluded that AggR autoactivates, creating a positive feedback loop (Morin et al., 2010). Although autoactivation ensures rapid stimulation and virulence factor production upon entry into conducive environments, positive feedback is potentially maladaptive to optimal bacterial growth by expelling the bacteria before the optimal bacterial load is reached (Santiago *et al.*, 2014) Therefore, AggR likely also uses a negative feedback regulator.

Morin *et al.* found an additional hypothetical protein in the AggR regulon that lacked homology to any characterized proteins (Morin et al., 2013). Santiago *et al.* conducted multiple sequence alignments to determine if this hypothetical protein was present in other species (Santiago et al., 2014). As seen in Figure 1, the hypothetical protein is found in *E. coli* pathotypes (EHEC, EPEC, STEC, ETEC, EIEC, EAEC) and other pathogenic bacterial species(Santiago et al., 2014). This hypothetical protein is termed AggR-activated regulator

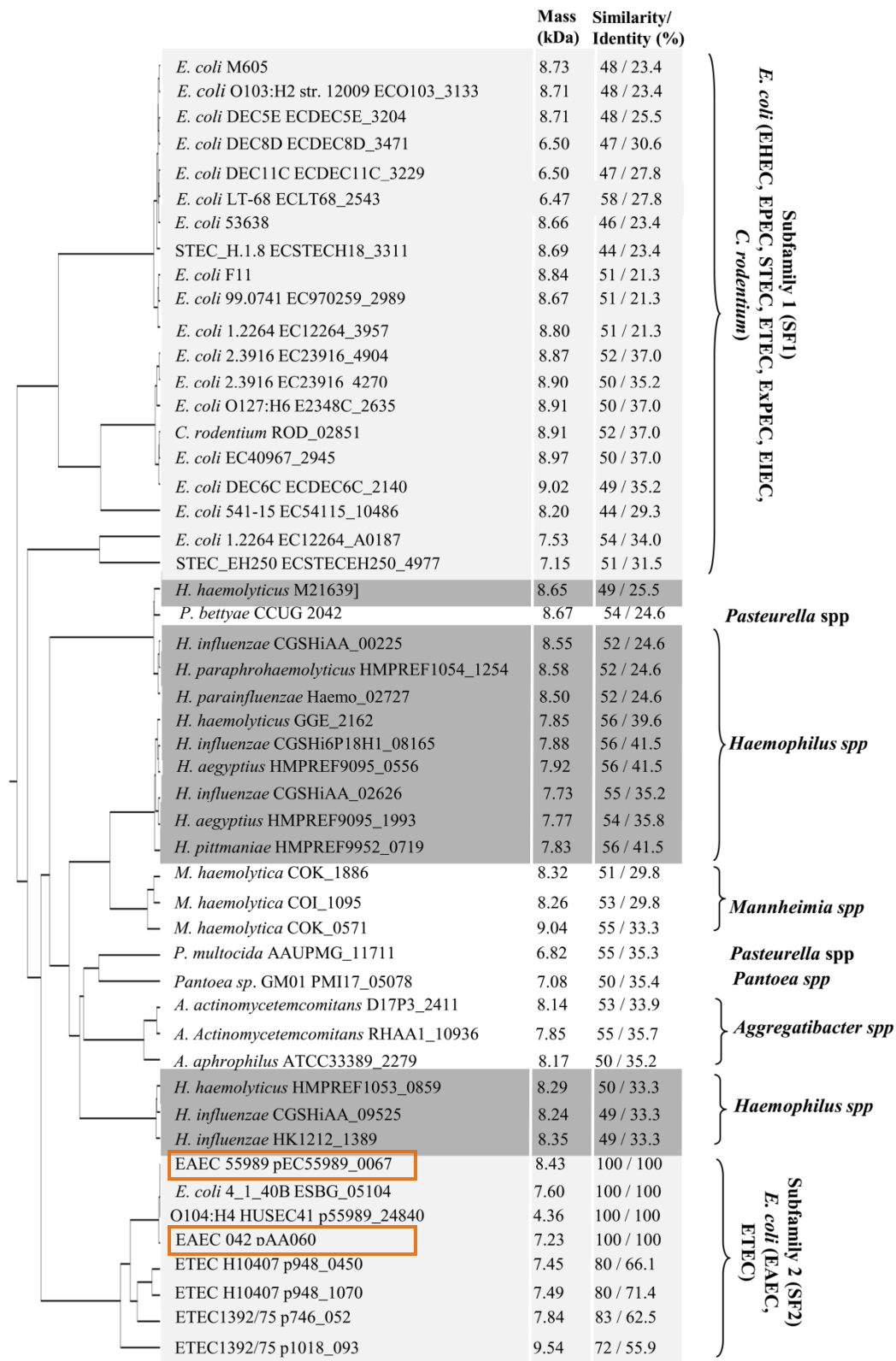


**Figure 1.** Phylogenetic analysis using ClustalW in various pathogenic species. EAEC species are highlighted in orange. Adapted figure (Santiago *et al.*, 2014).

(Aar), and is hypothesized to be the AggR negative regulator(Santiago et al., 2014). Recent work shows that Aar RNA levels are upregulated by AggR (Santiago *et al.*, 2014). Santiago *et al.* studied the relationship between AggR upregulation and Aar upregulation. The data indicate that AggR expression and Aar expression are inversely related (Santiago et al., 2014). From these data, three mechanisms of control are likely: i) Aar binds DNA, thus occluding a specific DNA sequence from AggR ii) Aar binds directly to AggR, thereby either changing the conformation of AggR, or blocking the AggR DNA binding site iii) Aar indirectly influences AggR through an unknown intermediate. Unpublished surface plasmon resonance (SPR) data suggests that there is a direct interaction between AggR and Aar. However, no structural data exists to validate the mechanism of inhibition.

Aar is attracting increased attention from the global health community due to its virulence regulation potential. This work provides a valid purification strategy for Aar from other contaminants and fusion partners. Furthermore, there is preliminary secondary structure information of Ubiquitin-Aar. Additional investigations are being conducted to elucidate the three-dimensional, high resolution structure. Structural data could theoretically lead to a regulatory loop, decreasing prevalence and pathogenicity of EAEC and other pathogens in children.

## Materials and Methods

### *Transformation and Cell Lysis – Ubiquitin-Aar/Aar-Ubiquitin*

BL21 (DE3) supercompetant cells were used for all transformations in these experiments. Cultures in Luria broth (LB) were induced at 37 degrees Celsius with IPTG at an  $OD_{600} = 0.6-0.8$ . Once induced for 4 hours, cells were centrifuged at 4,000 rpm for 10 minutes and frozen at -80 degrees Celsius for 16 hours. The pellet was resuspended in histidine binding buffer (HBB) (10mM  $NaH_2PO_4$ , pH 8.0, 0.3M NaCl, 10mM Imidazole, 1mM PMSF). Sonication was performed on ice with the FB120 Sonicator (Fisher Scientific) (100 percent intensity, 10 second intervals, 30 seconds/mL). The lysate was then centrifuged for 30 minutes at 14,000 rpm.

### *Purification— Ubiquitin-Aar*

The protein was purified using standard  $Ni^{2+}$  procedures (Rudloff, Woosley, & Wright, 2015). The cell lysate was passed over  $Ni^{2+}$  column, equilibrated in HBB and washed with 5 column volumes of histidine wash buffer (HWB) (10mM  $NaH_2PO_4$ , pH 8.0, 0.3M NaCl, 60mM Imidazole, 1mM PMSF). The protein was eluted in histidine elution buffer (HEB) (10mM  $NaH_2PO_4$ , pH 8.0, 0.3M NaCl, .25M Imidazole). The flow through (FT) was then collected, diluted (1:10) and loaded onto a sulfopropyl (S) column. FT was discarded and the column was washed with three column volumes (10mM  $NaH_2PO_4$ , pH 8.0, 25mM NaCl). The protein was eluted in 15 mL of elution buffer (10mM  $NaH_2PO_4$ , pH 8.0, 200mM NaCl and 10mM  $NaH_2PO_4$ , pH 8.0, 500mM NaCl, respectively), collected and concentrated at 4,000 rpm for 90 minutes in a swinging bucket centrifuge using a Spin-X UF concentrator (Corning) (10k MWCO PES).

### *Circular Dichroism – Ubiquitin-Aar*

Circular dichroism was performed on J-810 spectropolarimeter (Jasco). All CD experiments were conducted in a 1 mm pathlength cuvette at 5 $\mu$ M protein (50mM  $NaPO_4$ , 250

mM NaCl). Spectra were collected at pH 7.0 and pH 7.5. Ubiquitin samples were obtained from the Berndsen laboratory at James Madison University.

#### *Transformation and Cell Lysis – Aar-MBP*

Cells were obtained from the Nataro laboratory at the University of Virginia. The bacteria containing the MBP-Aar construct was grown and lysed according to the pMAL™ Protein Fusion and Purification Manual. Transformed cells were grown in rich Luria broth + glucose (2g/L) to an OD<sub>600</sub> = 0.6-0.8 and induced with IPTG. Once induced, cells were incubated for 4 hours, centrifuged at 4,000 rpm for 10 minutes and then frozen at -20 degrees Celsius overnight. The pellet was resuspended in column buffer (CB)(20mM Tris-HCl, pH 7.5, 200mM NaCl, 1 mM EDTA, 1mM PMSF) and sonicated using the FB120 Sonicator (Fisher Scientific) (75% intensity ,10 second intervals, 1 minute/mL).

#### *Purification – Aar-MBP*

Purification was done using the pMAL™ Protein Fusion and Purification Manual (New England BioLabs, Inc., 2015). The crude extract was diluted 1:6 using CB and loaded onto an amylose column (New England BioLabs, Inc.). The column was washed with 5 column volumes of CB and eluted with 15 mL of MBP elution buffer (20mM Tris-HCl, pH 7.5, 200mM NaCl, 1 mM EDTA, 10mM maltose). The sample was concentrated at 4,000 rpm for 90 minutes using the Spin-X UF Concentrator (5k MWCO PRES) and cleaved with Factor Xa (1% w/w ratio of final protein weight) (New England BioLabs, Inc.). Cleavage was performed at 4 degrees Celsius for 8 hours in CB. The protein was then loaded onto a Superdex75 column (20mM Tris-HCl, pH 7.5, 200mM NaCl, 1mM EDTA).

*MS/HPLC – Aar-MBP*

Prior to size exclusion on the SuperdexG75 column, protein samples were passed over a G-25 column using Low salt buffer (10mM NaCl, 10 mM  $\text{NH}_4\text{C}_2\text{H}_3\text{O}_2$ ). Samples were separated using the 1290 Infinity HPLC system (Agilent Technologies) using a 5-90% acetonitrile in water gradient with 0.1% formic acid and a Biobasic 18 HPLC column. (ThermoFisher). The column compartment was equilibrated to 50 degrees Celsius and absorbances were taken at 280nm. Mass spectrometry spectra were obtained 8530 Accurate-Mass Q-TOF LC/MS (Agilent Technologies).

## Results

### *SDS-PAGE gel electrophoresis*

One hypothesis at the inception of the project proposed that Aar was a transcription factor, suggesting that it is likely short-lived within the cell. Additionally, whole cell assays did not contain any evidence of a protein Aar's size. Aar was covalently linked to fusion partners to enhance stability and expression. Various purification strategies including centrifugation and affinity

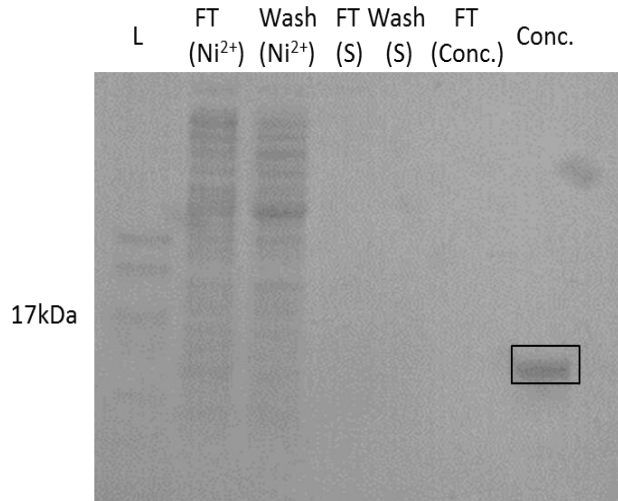
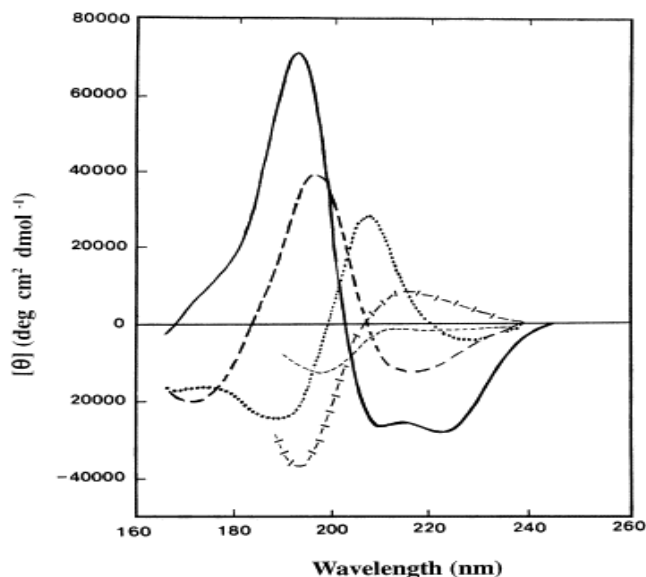


Figure 2. SDS-PAGE gel of Ubiquitin-Aar after purification on nickel ( $\text{Ni}^{2+}$ ) and sulfopropyl resin. Pure Ubiquitin-Aar can be visualized around the 17 kDa standard in the final lane.

chromatography were used to purify Ubiquitin-Aar. The  $\text{Ni}^{2+}$  column flow through (Figure 2, lane 2) and  $\text{Ni}^{2+}$  wash (Figure 2, lane 3) contained many different protein bands. Additional purification steps including a sulfopropyl column and centrifugation resulted in a single faint band around the expected molecular weight (17.9 kDa) (Figure 2, lane 7). Pure, full-length Ubiquitin-Aar was subjected to further experimentation to determine the secondary structure.

### *Circular Dichroism*

Circular dichroism (CD) was employed to analyze the secondary structure of Ubiquitin-Aar. Differential absorbance of left and right polarized UV light by chiral centers was used to identify fundamental protein secondary structures (Figure 3). The solid line (Figure 3) is representative of  $\alpha$ -helical structure, while the long dashed line (Figure 3) delineates a predominately  $\beta$ -sheet structure and the short dashed line (Figure 3) is representative of irregular



**Figure 3.** Far UV circular dichroism (CD) associated with different secondary structures. Solid line:  $\alpha$ -helix, long dashed line: type I  $\beta$ -turn; cross dashed line: poly (Pro) II helix; short dashed line: irregular structure.  $\alpha$ -helical spectra are characterized by negative bands at 222nm and 208nm, while  $\beta$ -sheet spectra show a negative band at 218nm. Adapted figure (Kelly, Jess, & Price, 2005).

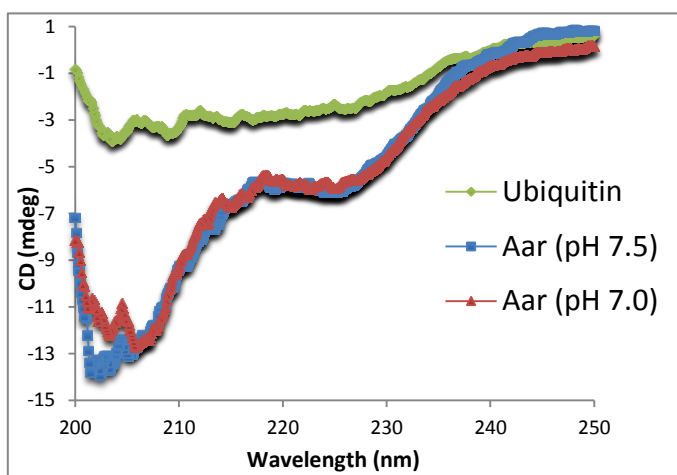


**Figure 4.** CD spectra for Ubiquitin and Ubiquitin-Aar complexes (pH 7.0 and pH 7.5, respectively). Differential absorbance readings were taken within the 200 to 250 nm range. Tests were done in triplicate and averaged.

structure. The differential absorption results in a spectrum that is representative of the conserved peptide backbone geometries associated with protein secondary structures. The collected Ubiquitin spectrum was compared to published data spectrum (Larios, Li, Schulten, Kihara, & Gruebele, 2004).

Although the signal to noise ratio was high in the current data, the Larios *et al.* profile is comparable to the collected Ubiquitin spectrum (3-10 $\mu$ M and 5 $\mu$ M, respectively) (Larios et al., 2004). CD experiments were then conducted on Ubiquitin-Aar to determine structural characteristics.

The introduction of Aar bound to Ubiquitin (Figure 4, red & Figure 4, blue) changed the absorbance spectra markedly from monomeric Ubiquitin (Figure 4, green), resulting in two characteristic peaks at 208 and 222 nm (Figure 4, red & Figure 4, blue). Qualitatively, the peaks suggest



the presence of a predominately alpha-helical structure as opposed to the random coil spectrum for Ubiquitin (Figure 4, green). Unpublished data by the Berndsen laboratory suggests Ubiquitin is denatured when sonicated above 30% intensity, suggesting the spectra for Ubiquitin-Aar (pH 7.0) (Figure 4, red) and Ubiquitin-Aar (pH 7.5) (Figure 4, blue) are not substantially altered by the presence of ubiquitin. There are potential intramolecular chemical interactions between Ubiquitin and Aar, likely slightly altering the spectra. Due to potential artifacts in the data and unsuccessful cleavage, Aar covalently linked to maltose binding protein (MBP) was used for all subsequent purification experiments.

#### *Purification – MBP-Aar*

Experiments to cleave Aar from its fusion partner Ubiquitin were unsuccessful. Due to the availability, stability and purification ease, MBP was used as a fusion partner for further testing. Various experiments including size exclusion chromatography and HPLC/MS were conducted to purify the construct. The protein samples were subjected to HPLC/MS peptide mapping after chromatography purification to confirm cleavage. The mass spectra for peptide identification were calculated manually to ensure accuracy. After deconvolution of multiply-charged ion series, the uncleaved MBP-Aar sample had single peak (Figure 5A). The experimental molecular mass, 52.1 kDa ( $m/z$  1.022) (Figure 5A), was compared to its theoretical molecular mass, 51.0 kDa, confirming the presence of uncleaved MBP-Aar. Cleaved MBP-Aar was also subjected to HPLC/MS analysis. Two variants of Aar, Aar-monomer and Aar-dimer, eluted in two distinct HPLC peaks (Figure 5B). The experimental molecular mass of Aar-monomer, 8.4 kDa ( $m/z$  ratio 1.091)(Figure 5A), was compared to its theoretical molecular mass, 8.5 kDa. Another peak was present in the spectrum (Figure 5B). Deconvolution revealed a species with a molecular weight of 16.8 kDa (Figure 5B), suggesting the formation of an Aar

dimer. Smaller peaks also exist in the spectrum around 30 seconds (Figure 5A, Figure 5B), however these peaks are the result of an overloaded column and had no effect on data acquisition and analysis. Once cleavage was confirmed, other chromatographic techniques were utilized to separate monomeric Aar from dimeric Aar and MBP.

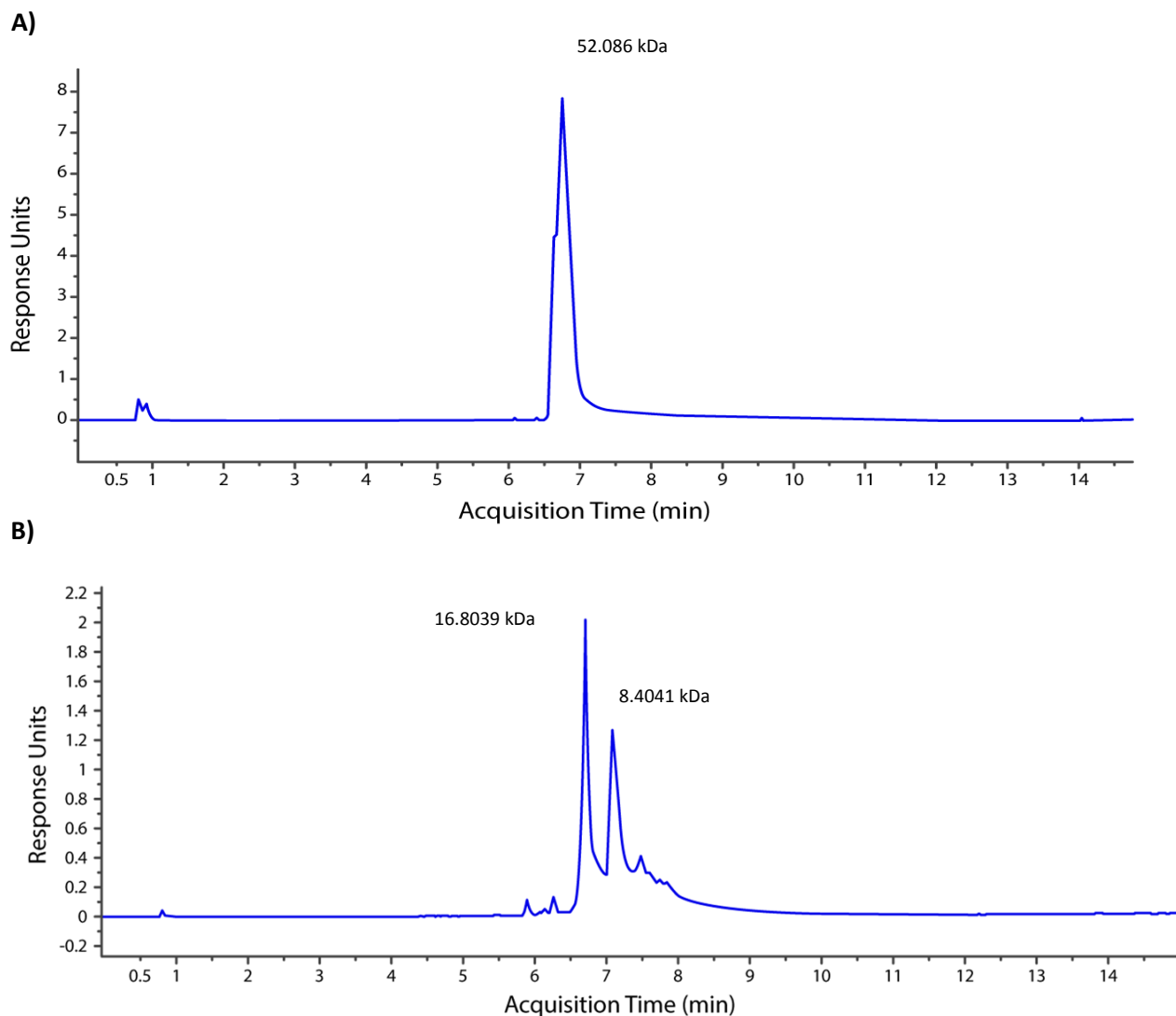


**Figure 5.** Chromatic separation when a 5-90 & acetonitrile gradient in water was used with 0.1% formic acid as the organic mobile phase. Analytes: (A) MBP-Aar (B) Aar (dimer), Aar (monomer).

Size chromatography was utilized to separate high molecular weight species from low molecular weight species. Fractions from the sizing column were selected based on OD<sub>280</sub>

absorbances (Figure 6A). Selected samples were run on an SDS-PAGE gel to determine purity. Lanes 36, 44 and 46 (Figure 6B) contained MBP and other contaminants, while lanes 49 and 56 (Figure 6B) contained pure MBP. Lane 62 (Figure 6B) contains a single faint band around 7.4kDa, the predicted molecular weight of monomeric Aar, suggesting that pure, monomeric Aar was obtained.

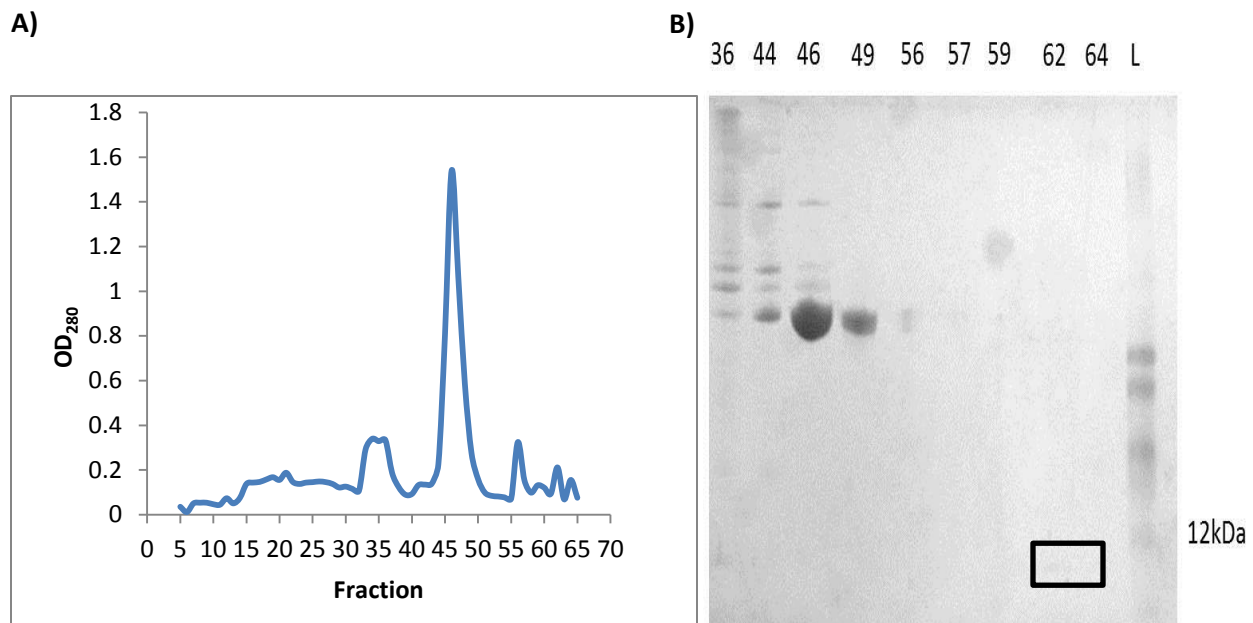


**Figure 6.** A) Size exclusion absorbance profiles for cleaved Aar-MBP. B) SDS-PAGE gel electrophoresis corresponding to the fractional data. Fraction 62 contains pure, dilute Aar-monomer.

## Discussion

Here, we present viable strategies for the purification of Aar from fusion partners, Ubiquitin and MBP. Using chromatographic methods (e.g affinity chromatography and size exclusion chromatography), Aar and its fusion proteins were purified from other cellular proteins. We expect that this purification strategy can be used to purify isotopically labeled Aar to study three-dimensional structural characteristics.

Aar was covalently linked to Ubiquitin due to the hypothesized ephemeral nature of Aar at physiological conditions. Purification experiments were successful (Figure 2, lane 7), but cleavage was not attainable. Unsuccessful cleavage was unexpected because the Ubiquitin-Aar construct contained a linear epitope recognized by the TEV protease. Unsuccessful cleavage is likely the result of either serine protease inhibitors (PMSF) present in the sample, an occluded active site due to conformational restrictions, or denaturation due to sonication. We cannot comment on the validity of Ubiquitin-Aar cleavage with TEV because the experiments were not conducted with pure protein. Since MBP-Aar cleaved, a valid cleavage strategy for Ubiquitin-Aar was not pursued.

Purification and cleavage experiments were conducted on MBP-Aar. To confirm cleavage of MBP-Aar, HPLC/MS (Q-TOF) was conducted. There is evidence of full length MBP-Aar (Figure 5, A), dimerized Aar and monomeric Aar (Figure 5, B). The experimental molecular weight, 8.4kDa, did not coincide with the predicted molecular weight. The disparity in molecular weight is likely due to discrepancies between the sequence used for prediction, Ubiquitin-Aar, and the sequencing information generated by the Nataro laboratory. However, the calculated difference, 0.1 kDa, between the theoretical molecular weight and the experimental molecular weight is likely the result of an additional amino acid in the Ubiquitin-Aar sequence.

Several other artifacts are present in the HPLC/MS spectra.

Both HPLC/MS spectra (Figure 5, A and B) contain other insignificant peaks. The Aar HPLC/MS spectrum contains additional peaks around six minutes (Figure 5, A and B). Thorough analysis was not conducted on these species, but m/z ratios suggested the presence of fragmented protein. Furthermore, the spectra do not have any species around 42.5 kDa, the theoretical molecular weight of MBP. These peaks were expected because separation did not occur until after HPLC/MS was conducted. The absence of MBP in the spectrum is likely the result of precipitation during the cleavage process. Although MBP was absent from the spectra, the precursors and final product were present, proving that successful cleavage occurred. Once cleavage was confirmed, measures were taken to separate Aar from dimeric Aar and MBP.

We have established a viable purification strategy for Aar using MBP as a fusion partner. Isotopically-labeled Aar is being purified for future studies, likely leading to high resolution structure through multi-dimensional NMR. There is evidence that Aar binds to AggR. However, there is no structural data to validate the binding mechanism. Future experiments will investigate physical interactions between Aar residues and AggR residues. Controlling this pathway through synthetic or natural methods could lead to novel pharmaceuticals, protecting kids from pathogenic species such as EAEC.

## References

- Boisen, N., Hansen, A., Melton-celsa, A. R., Zangari, T., Mortensen, N. P., Kaper, J. B., ... Nataro, J. P. (2014). The Presence of the pAA Plasmid in the German O104 : H4 Shiga Toxin Type 2a ( Stx2a ) – Producing Enteroaggregative Escherichia coli Strain Promotes the Translocation of Stx2a Across an Epithelial Cell Monolayer, *210*, 1909–1919. doi:10.1093/infdis/jiu399
- Centers for Disease Control and Prevention. (2014). *E. coli (Escherichia coli)*. Retrieved from <http://www.cdc.gov/ecoli/general/>
- Kaper, J. B., Nataro, J. P., & Mobley, H. L. (2004). Pathogenic escherichia coli. *Nature Reviews Microbiology*, *2*(2), 123-140.
- Kelly, S. M., Jess, T. J., & Price, N. C. (2005). How to study proteins by circular dichroism. *Biochimica et Biophysica Acta - Proteins and Proteomics*, *1751*, 119–139. doi:10.1016/j.bbapap.2005.06.005
- Larios, E., Li, J. S., Schulten, K., Kihara, H., & Gruebele, M. (2004). Multiple probes reveal a native-like intermediate during low-temperature refolding of ubiquitin. *Journal of Molecular Biology*, *340*, 115–125. doi:10.1016/j.jmb.2004.04.048
- Morin, N., Santiago, A. E., Ernst, R. K., Guillot, S. J., & Nataro, J. P. (2013). Characterization of the AggR regulon in enteroaggregative Escherichia coli. *Infection and Immunity*, *81*(1), 122–132. doi:10.1128/IAI.00676-12
- Morin, N., Tirling, C., Ivison, S. M., Kaur, A. P., Nataro, J. P., & Steiner, T. S. (2010). Autoactivation of the AggR regulator of enteroaggregative Escherichia coli in vitro and in vivo. *FEMS Immunology and Medical Microbiology*, *58*, 344–355. doi:10.1111/j.1574-695X.2010.00645.x
- Nataro, J. P., Yikang, D., Yingkan, D., & Walker, K. (1994). AggR, a transcriptional activator of aggregative adherence fimbria I expression in enteroaggregative Escherichia coli. *Journal of Bacteriology*, *176*(15), 4691–4699.
- New England BioLabs, Inc. PMAL protein fusion & purification system. (2015, January 15).
- Rudloff, M.W., Woosley, A.N., Wright, N.T. (2015). Biophysical characterization of naturally occurring titan M10 mutations. *Protein Science: A Publication Of The Protein Society*, doi:10.1002/pro.2670
- Santiago, A. E., Ruiz-Perez, F., Jo, N. Y., Vijayakumar, V., Gong, M. Q., & Nataro, J. P. (2014). A Large Family of Antivirulence Regulators Modulates the Effects of Transcriptional Activators in Gram-negative Pathogenic Bacteria. *PLoS Pathogens*, *10*(5), e1004153. doi:10.1371/journal.ppat.1004153

- Sarantuya, J., Nishi, J., Wakimoto, N., Nataro, J. P., Sheikh, J., Manago, K., ... Iwashita, M. (2004). Typical Enteroaggregative Escherichia coli Is the Most Prevalent Pathotype among E . coli Strains Causing Diarrhea in Mongolian Children Typical Enteroaggregative Escherichia coli Is the Most Prevalent Pathotype among E . coli Strains Causing Diarrhea in . *Society*, *42*(1), 133–139. doi:10.1128/JCM.42.1.133
- Stark, R. L., & Duncan, C. L. (1972). Transient Increase in Capillary Permeability Induced, *5*(1), 147–150.
- Van Den Beld, M. J. C., & Reubsaet, F. a G. (2012). Differentiation between Shigella, enteroinvasive Escherichia coli (EIEC) and noninvasive Escherichia coli. *European Journal of Clinical Microbiology and Infectious Diseases*, *31*, 899–904. doi:10.1007/s10096-011-1395-7
- World Health Organization. (2014). *Diarrhoeal disease*. Retrieved from <http://www.who.int/mediacentre/factsheets/fs330/en/>

## **Supplemental Methods**

### *X-ray Crystallography*

Preceding cleavage, MBP-Aar crystal screens were set using Index 1, Index 2, PEGRx1, PEGRx2, Natrix1, Natrix 2, and PEG/Ion solution screens (Hampton Research). Screens were set using the hanging drop vapor diffusion method at 26 degrees Celsius. Two  $\mu$ Ls of protein solution (10mg/mL) were mixed with 2  $\mu$ Ls of well solution.

## **Supplemental Results**

### *X-ray Crystallography*

Crystal trays were set using full length MBP-Aar. Condition 64 (0.005M Cobalt(II), 0.005M Nickle(II), 0.005 cadmium chloride hydrate, 0.005M magnesium chloride hydrate, 0.1M HEPES, pH 7.5, 12% w/v PEG 3350) (Index 2) contained granular precipitate. Multiple wells were set, but only granular crystals have formed. Future experiments should optimize the condition for three-dimensional (3D) crystals.